



## Effects of heat generation and thermal radiation on steady MHD flow near a stagnation point on a linear stretching sheet in porous medium and presence of variable thermal conductivity and mass transfer

S. Mohammed Ibrahim<sup>a,\*</sup> and K. Suneetha<sup>a</sup>

<sup>a</sup> Department of Mathematics, Priyadarshini College of Engineering and Technology, Nellore, Andhra Pradesh, India - 524004

---

### Article info:

Received: 17/01/2014  
Accepted: 12/06/2014  
Online: 03/03/2015

---

### Keywords:

Boundary layer,  
Steady,  
MHD,  
Stagnation point,  
Radiation,  
Mass transfer,  
Porous medium,  
Heat generation.

### Abstract

The present paper was aimed to study the effects of variable thermal conductivity and heat generation on the flow of a viscous incompressible electrically conducting fluid in the presence of a uniform transverse magnetic field, thermal radiation, porous medium, mass transfer, and variable free stream near a stagnation point on a non-conducting stretching sheet. Equations of continuity, momentum, energy, and mass were transformed into ordinary differential equations and solved numerically using shooting method. Velocity, temperature, and concentration distributions were numerically discussed and presented in the graphs. Skin-friction coefficient, the Nusselt number, and Sherwood number on the sheet were derived and discussed numerically. Their numerical values for various values of physical parameters were presented in the tables. It was found that temperature increased with increasing radiation parameter,  $R$ , and concentration decreased with increasing the Schmidt number,  $Sc$ . The numerical predications were compared with the existing information in the literature and a good agreement was obtained.

---

### 1. Introduction

In fluid dynamics, effects of external magnetic field on magneto hydrodynamic (MHD) flow over a stretching sheet are very important because of applications in many engineering problems, such as glass manufacturing, geophysics, paper production, and crude oil purification. The flow related to the stretching of a flat surface was first investigated by Crane [1]. Pavlov [2] studied the effect of external magnetic field on the MHD flow over a

stretching sheet. Andersson [3] discussed the MHD flow of viscous fluid on a stretching sheet. Mukhopadhyay et al. [4] presented the MHD flow and heat transfer over a stretching sheet with variable fluid viscosity. Bhattacharyya and Layek [5] showed the behavior of solute distribution in the MHD boundary layer flow past a stretching sheet. Furthermore, many vital properties of MHD flow over stretching sheet have been explored in articles [6- 8] in the related literature.

---

\*Corresponding author

Email address: [ibrahimsvu@gmail.com](mailto:ibrahimsvu@gmail.com)

The field of boundary layer flow problem over a stretching sheet has many industrial applications, such as in polymer sheet, filament extrusion from a dye, long thread between feed roll or wind-up roll, glass fiber and paper production, drawing of plastic films, and liquid films in condensation process. Due to the high applicability of this problem in such industrial phenomena, it has attracted the attentions of many researchers. Sakiadis [9] was the first who studied boundary layer flow over a stretching surface moving at constant velocity in an ambient fluid. He employed a similarity transformation and obtained a numerical solution for the problem. Erickson *et al.* [10] extended the work of Sakiadis [9] to account for mass transfer on the stretching surface. Tsou *et al.* [11] presented a combined analytical and experimental study on the flow and temperature field in the boundary layer on a continuous moving surface. Noghrehabadi *et al.* [12] studied the effect of partial slip boundary conditions on the flow and heat transfer of nanofluids past stretching sheet prescribed constant wall temperature. Noghrehabadi *et al.* [13] analyzed the flow and heat transfer of nanofluid over stretching sheet while taking into account particle slip and thermal convective boundary conditions.

The stagnation point flows are classic problems in the field of fluid dynamics and have been investigated by many researches. These flows can be viscous or in viscid, steady or unsteady, two-dimensional or three-dimensional, normal or oblique, and forward or reverse. The steady flow in the neighborhood of a stagnation point was first studied by Hiemenz [14], who used a similarity transformation to reduce the Navier-Stokes equations to nonlinear ordinary differential equations. This problem was extended by Homann [15] to the case of axisymmetric stagnation point flow. Stagnation point flows have been discussed by Pai [16], Schlichting [17], Bansal [18], Chiam [19], etc. Mahapatra and Gupta [20] and Nazar *et al.* [21] have investigated the heat transfer in the steady two-dimensional stagnation point flow of a viscous fluid by taking different aspects into account.

Kay [22] proposed that thermal conductivity of liquids with low Prandtl number varied linearly with temperature in the range of 0 to 400°F. Arunachalam and Rajappa [23] considered forced convection in liquid metals (i.e. fluid with low Prandtl number) with variable thermal conductivity and capacity in the potential flow and derived an explicit closed form of analytical solution. Fluid flow and heat transfer characteristics on stretching sheet with variable temperature conditions were investigated by Grubka and Bobba [24]. Chaim [25] studied heat transfer in the fluid flow of low Prandtl number with variable thermal conductivity induced as a result of stretching sheet and compared the numerical results with the perturbation solution.

Effect of thermal radiation on flow and heat transfer processes is of major importance in the design of many advanced energy conversion systems operating at high temperature. Thermal radiation within such systems occurs because of the emission by the hot walls and working fluid. Pop *et al.* [26] discussed the flow over stretching sheet near a stagnation point while considering thermal radiation effect. The effect of radiation on heat transfer problems was studied by Hossain and Takhar [27]. Pal [28] investigated heat and mass transfer in stagnation point flow towards a stretching surface in the presence of buoyancy force and thermal radiation. Vyas and Srivastava [29] presented a numerical study for the steady two-dimensional radiative MHD boundary layer, with a reference to the flow of an incompressible, viscous, and electrically conducting fluid caused by a non-isothermal linearly stretching sheet placed at the bottom of a fluid saturated porous medium.

The study of heat generation or absorption in moving fluids is important in the problems dealing with chemical reactions and those concerned with dissociating fluids. Possible heat generation effects may alter temperature distribution, which may influence particle deposition and distribution rate; hence, the particle deposition and distribution rate in the conductor wafers. The steady hydromagnetic laminar stagnation point flow of an

incompressible viscous fluid impinging on a permeable stretching surface with heat generation or absorption was analyzed by Attia [30]. Sharma and Singh [31] investigated the effects of variable thermal conductivity and heat source/sink on flow near a stagnation point on a non-conducting stretching sheet. Effects of variable thermal conductivity and heat source/sink on steady two-dimensional radiative MHD boundary layer flow of a viscous, incompressible, and electrically conducting fluid in the presence of variable free stream near a stagnation point on a non-conducting stretching sheet was investigated by Al-Sudais [32]. Noghrehabadi et al. [33] analyzed the boundary layer heat transfer and entropy generation of a nanofluid over an isothermal linearly stretching sheet with heat generation/absorption.

The objective of this study was to extend the work by Al-Sudais [32], considering the mass transfer. The governing equations were transformed using similarity transformation and the resultant dimensionless equations were solved numerically using the Runge-Kutta fourth order method by shooting technique. The effects of various governing parameters on the velocity, temperature, concentration, skin-friction coefficient, the Nusselt number, and Sherwood number are shown in figures and tables and analyzed in detail. To the best knowledge of the present authors, this problem has not been studied before.

**2. Formulating the problem**

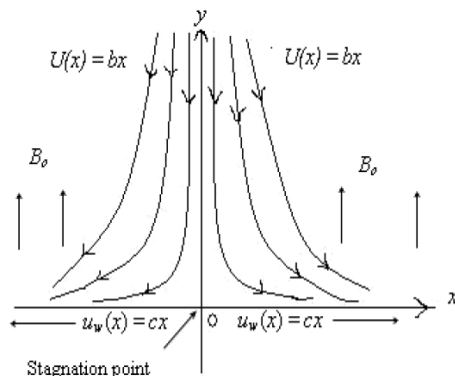


**Fig. 1.** Sketch of the physical model.

Consider a steady two-dimensional flow of viscous incompressible electrically conducting fluid with variable thermal conductivity in the vicinity of a stagnation point on a non-conducting stretching sheet in the presence of transverse magnetic field and volumetric rate of heat generation. The stretching sheet has uniform temperature,  $T_w$ , and linear velocity,  $u_w(x)$ . It is assumed that external field is zero and the electric field owing to the polarization of charges and Hall effect is neglected. Stretching sheet is placed in the plane  $y = 0$  and  $x$ -axis is taken along the sheet, as shown in Fig. 1. The fluid occupies the upper half plane i.e.  $y > 0$ . The governing equations of continuity, momentum, energy, and concentration under the influence of externally imposed transverse magnetic field (Bansal [18]) with variable thermal conductivity in the boundary layer are:

$$\frac{\partial u}{\partial x} + \frac{\partial v}{\partial y} = 0 \tag{1}$$

$$u \frac{\partial u}{\partial x} + v \frac{\partial u}{\partial y} = -\frac{1}{\rho} \frac{\partial p}{\partial x} + \nu \frac{\partial^2 u}{\partial y^2} - \frac{\sigma B_0^2}{\rho} u - \frac{\nu}{K^*} u \tag{2}$$

$$\rho c_p \left( u \frac{\partial T}{\partial x} + v \frac{\partial T}{\partial y} \right) = \frac{\partial}{\partial y} \left( k^* \frac{\partial T}{\partial y} \right) - \frac{\partial q_r}{\partial y} + Q^* (T - T_\infty) \tag{3}$$

$$u \frac{\partial C}{\partial x} + v \frac{\partial C}{\partial y} = D \frac{\partial^2 C}{\partial y^2} \tag{4}$$

where  $x$  and  $y$  represent the coordinate axes along the continuous stretching surface in the direction of motion and normal to it, respectively;  $u$  and  $v$  are the velocity components along the  $x$  and  $y$  axes, respectively;  $p$  is the pressure of the fluid;  $\nu$  is the kinematic viscosity;  $\sigma$  is electrical conductivity;  $B_0$  is the magnetic field intensity;  $\rho$  is the fluid density;  $K^*$  is the permeability of the porous medium;  $c_p$  is the specific heat at

constant pressure;  $q_r$  is the radiation heat flux;  $T$  is the fluid temperature;  $T_\infty$  is the fluid free stream temperature;  $T_w$  is the fluid temperature of stretching sheet;  $C$  is the fluid concentration;  $C_\infty$  is the fluid free stream concentration;  $C_w$  is the fluid concentration of stretching sheet;  $k^*$  is the variable thermal conductivity;  $Q^*$  is the volumetric rate of heat generation; and  $D$  is the molecular diffusivity of the species concentration.

The second derivatives of  $u$  and  $T$  with respect to  $x$  are eliminated on the basis of magnitude analysis considering that Reynolds number is high. Hence, the Navier-Stokes equation is modified into Prandtl's boundary layer equation.

In the free stream  $u = U(x) = bx$ , Eq. (2) is reduced to:

$$U \frac{dU}{dx} = -\frac{1}{\rho} \frac{\partial p}{\partial x} - \frac{\sigma B_0^2}{\rho} U \tag{5}$$

By eliminating  $\frac{\partial p}{\partial x}$  between Eqs. (2 and 5), the following is obtained:

$$u \frac{\partial u}{\partial x} + v \frac{\partial u}{\partial y} = U \frac{dU}{dx} + v \frac{\partial^2 u}{\partial y^2} - \frac{\sigma B_0^2}{\rho} (u - U) - \frac{v}{K^*} u \tag{6}$$

The boundary conditions for the present problem are:

$$u = u_w(x) = cx, \quad v = 0, \quad T = T_w, \quad C = C_w \text{ at } y = 0,$$

$$u = U(x) = bx, \quad T = T_\infty, \quad C = C_\infty \text{ as } y \rightarrow \infty. \tag{7}$$

Using the Rosseland approximation for radiation (Brewster [34]), the radiative heat flux  $q_r$  could be expressed by:

$$q_r = -\frac{4\sigma^*}{3k_0} \frac{\partial T^4}{\partial y} \tag{8}$$

where  $\sigma^*$  represents the Stefan-Boltzman constant and  $k_0$  is the Rosseland mean absorption coefficient. By assuming that the

temperature difference within the flow is such that  $T^4$  may be expanded in a Taylor series about  $T_\infty$  and neglecting higher orders, the following is obtained:

$$T^4 \cong 4T_\infty^3 T - 3T_\infty^4 \tag{9}$$

Following Arunachalam and Rajappa [23] and Chaim [25], thermal conductivity  $k^*$  is taken with the form as given below:

$$k^* = k(1 + \varepsilon\theta) \tag{10}$$

The continuity Eq. (1) is satisfied by introducing the stream function  $\psi(x, y)$  such that:

$$u = \frac{\partial \psi}{\partial y} \text{ and } v = -\frac{\partial \psi}{\partial x}.$$

The following non-dimensional variables are introduced:

$$\psi(x, y) = (cv)^{\frac{1}{2}} xf(\eta), \quad \eta = \left(\frac{c}{v}\right)^{\frac{1}{2}} y,$$

$$\theta(\eta) = \frac{T - T_\infty}{T_w - T_\infty}, \quad \phi(\eta) = \frac{C - C_\infty}{C_w - C_\infty}, \quad \lambda = \frac{b}{c}$$

$$K = \frac{v}{K^*c}, \quad M = \frac{\sigma B_0^2}{\rho c}, \quad R = \frac{16\sigma^* T_\infty^3}{3k_0 k},$$

$$\text{Pr} = \frac{\mu c_p}{k}, \quad Q = \frac{Q^*}{\rho c_p c}, \quad \text{Sc} = \frac{v}{D}. \tag{11}$$

Using Eqs. (8-11) in Eqs. (6, 3 and 4), the following ordinary differential equations can be obtained:

$$f''' + ff'' - f'^2 - M(f' - \lambda) - Kf' + \lambda^2 = 0, \tag{12}$$

$$(1 + R + \varepsilon\theta)\theta'' + \varepsilon\theta'^2 + \text{Pr} f\theta' + \text{Pr} Q\theta = 0 \tag{13}$$

$$\phi'' + \text{Sc} f\phi' = 0 \tag{14}$$

where the primes denote the differentiation with respect to  $\eta$ ,  $\lambda$  is the ratio of free stream velocity parameter to stretching sheet parameter,  $b$  is the free stream velocity parameter,  $c$  is the stretching sheet parameter,

$M$  is the magnetic parameter,  $K$  is the permeability parameter,  $Pr$  is the Prandtl number,  $R$  is the thermal radiation parameter,  $\varepsilon$  is perturbation parameter,  $Q$  is the heat generation parameter, and  $Sc$  is the Schmidt number.

The corresponding boundary conditions are reduced to:

$$\begin{aligned} f(0) = 0, \quad f'(0) = 1, \quad \theta(0) = 1, \quad \phi(0) = 1 \\ f'(\infty) = \lambda, \theta(\infty) = 0, \phi(\infty) = 0 \end{aligned} \quad (15)$$

### 3. Skin-friction coefficient, the Nusselt number and Sherwood number

In practical applications, three quantities of physical interest are to be determined, such as surface shear stress, rate of heat transfer, and rate of mass transfer on the surface. They may be obtained in terms of the skin friction coefficient:

$$C_f = \frac{\tau_w}{\rho c \sqrt{cv}} = xf''(0) \quad (16)$$

The local Nusselt number:

$$Nu = \left(\frac{v}{c}\right)^{\frac{1}{2}} \frac{q_w}{k^*(T_w - T_\infty)} = -\theta'(0) \quad (17)$$

and the local Sherwood number:

$$Sh = \left(\frac{v}{c}\right)^{\frac{1}{2}} \frac{m_w}{D(C_w - C_\infty)} = -\phi'(0) \quad (18)$$

where  $\tau_w = \mu \left(\frac{\partial u}{\partial y} + \frac{\partial v}{\partial x}\right)_{y=0}$  is the shear-stress along the sheet

$q_w = -k^* \left(\frac{\partial T}{\partial y}\right)_{y=0}$  is the surface heat transfer

rate, and  $m_w = -D \left(\frac{\partial C}{\partial y}\right)_{y=0}$  is the surface mass transfer rate.

### 4. Method of solution

The governing boundary layer, thermal and concentration boundary layer Eqs. (12-14) with the boundary conditions (15) are solved using

Runge-Kutta fourth order technique along with shooting method (Conte and Boor [35]). First of all, higher order non-linear differential Eqs. (12-14) are converted into simultaneous linear differential equations of order first and further transformed into initial value problem by the shooting technique. Once the problem is reduced to the initial value problem, it is solved using Runge-Kutta fourth order technique (Jain [36], Jain *et al.* [37], Krishnamurthy and Sen [38]).

### 5. Results and discussion

system of non-linear ordinary differential Eqs. (12-14) is solved numerically using shooting method for different values of magnetic field parameter,  $M$ , permeability of the porous medium,  $K$ , ratio of free stream velocity parameter to stretching sheet parameter,  $\lambda$ , thermal radiation parameter,  $R$ , the Prandtl number,  $Pr$ , heat generation parameter,  $Q$ , perturbation parameter,  $\varepsilon$ , and the Schmidt number,  $Sc$ .

In order to assess the accuracy of the numerical method, results for  $f''(0)$  in the absence of magnetic field parameter ( $M = 0$ ) are compared with those of Pop *et al.* [26], Mahapatra and Gupta [20], and Al-Sudais [32]. The first used Runge-Kutta fourth order method and shooting technique, while the second applied finite difference technique and Thomas algorithm; the last one used Runge-Kutta fourth order method along with shooting technique. The result of the comparison found a good agreement among them. These comparisons are shown in Table 1. It is seen from table 2 that the numerical values of  $-\theta'(0)$  in the present paper, when  $M = K = R = Q = Sc = \varepsilon = 0$  and  $Pr = 0.05$ , are in agreement with those obtained by Pop *et al.* [26], Mahapatra and Gupta [20], and Al-sudais [32].

To analyze the results, numerical computations are carried out for variations in the governing parameters such as magnetic field parameter,  $M$ , permeability of the porous medium,  $K$ , ratio of free stream velocity parameter to stretching sheet parameter,  $\lambda$ , thermal radiation parameter,  $R$ , the Prandtl number,  $Pr$ , heat

generation parameter,  $Q$ , perturbation parameter,  $\varepsilon$ , and the Schmidt number,  $Sc$ .

In the present study, the following default parameter values are adopted for computations:  $M = 0.1$ ,  $K = 0.1$ ,  $Pr = 0.71$ ,  $R = 1.0$ ,  $Q = 0.1$ ,  $\lambda = 0.1$ ,  $\varepsilon = 0.1$ ,  $Sc = 0.22$ .

All graphs therefore correspond to these values unless specifically indicated in the appropriate graph.

Figure 2 represents the importance of magnetic field for the velocity profiles. The presence of transverse magnetic field parameter  $M$  is set in Lorentz force, which results in retarding force on the velocity field. Therefore, as magnetic field parameter increases, so does the retarding force and hence the velocity profiles decrease, as shown in Figure 2. Figures 3 and 4 display the temperature and concentration profiles with magnetic field parameter, respectively. From these figures, it can be observed that both temperature and concentration profiles increase as magnetic field parameter increases.

The effect of the permeability of porous medium parameter,  $K$ , on velocity, temperature, and concentration profiles is shown in Figs. 5-7, respectively. It can be observed that velocity is reduced as the permeability of porous medium,  $K$ , increases, while temperature and concentration enhance as the permeability of porous medium,  $K$ , increases, which implies that the resistance of the medium is decreasing due to the increased restriction resulting from decreasing porosity of the porous medium.

Figure 8 illustrates the dimensionless temperature profiles for different values of the Prandtl number  $Pr$ . It is observed that an increase in the Prandtl number results in the decreased thickness of thermal boundary layer and in general lower average temperature within the boundary layer. The reason is that smaller values of the Prandtl number are equivalent to increasing the thermal conductivities; therefore, heat is able to diffuse away from the heated plate more rapidly than for higher values of  $Pr$ ; in the case of smaller Prandtl number, as the boundary layer is thicker, the rate of transfer is reduced.

Figure 9 predicts the influence of the radiation parameter,  $R$ , on temperature field. The

radiation parameter,  $R$ , defines the relative contribution of conduction heat transfer to thermal radiation transfer. It is obvious that an increase in the radiation parameter results in increasing temperature within the boundary layer.

Figure 10 shows the influence of the heat generation parameter,  $Q$ , on temperature profiles within the thermal boundary layer. From Figure 10, it is observed that the temperature increases with an increase in the heat generation parameter,  $Q$ .

Figure 11 represents the temperature profiles for some values of the perturbation parameter,  $\varepsilon$ , and for fixed values of all others. Figure 11 represents that, with the increase in the value of  $\varepsilon$ , temperature profiles increase the thermal conductivity constant, leading to lower approximation of the temperature profile.

For different values of the Schmidt number,  $Sc$ , the concentration profile is plotted in Fig. 12. The Schmidt number,  $Sc$ , embodies the ratio of the momentum diffusivity to the mass (species) diffusivity. It physically relates the relative thickness of the hydrodynamic boundary layer and mass transfer (concentration) boundary layer. As the Schmidt number,  $Sc$ , increases, the concentration decreases, which causes the concentration buoyancy effects to decrease and yield a reduction in the fluid velocity. The reduction in the concentration profiles is accompanied by simultaneous reductions in the concentration boundary layers, which is evident in Fig. 12.

Figure 13 depicts the ratio of free stream velocity parameter to stretching sheet parameter,  $\lambda$  in velocity profiles. It is clear that the velocity profiles increase with an increase in the values of parameter  $\lambda$ . Figures 14 and 15 show the temperature and concentration profiles for different values of the ratio of free stream velocity parameter to stretching sheet parameter,  $\lambda$ . It is observed in Figs. 14 and 15 that fluid temperature and concentration decreases due to increased  $\lambda$ .

Effects of various governing parameters on the skin-friction coefficient,  $C_f$ , the Nusselt number,  $Nu$ , and the Sherwood number,  $Sh$ , are

shown in Tables 3 and 4. It can be noticed that, as magnetic parameter  $M$  or permeability parameter  $K$  increase, the skin-friction coefficient increases and both Nusselt number and Sherwood number decrease. As  $\lambda$  increases, skin-friction coefficient is reduced, while the Nusselt number and Sherwood number increase. The Nusselt number increases

as the Prandtl number increases, while Nusselt number is reduced as thermal radiation parameter,  $R$ , heat generation parameter,  $Q$ , or perturbation parameter,  $\varepsilon$ , increases. It is seen that the Sherwood number increases as an increase in the Schmidt number,  $Sc$ .

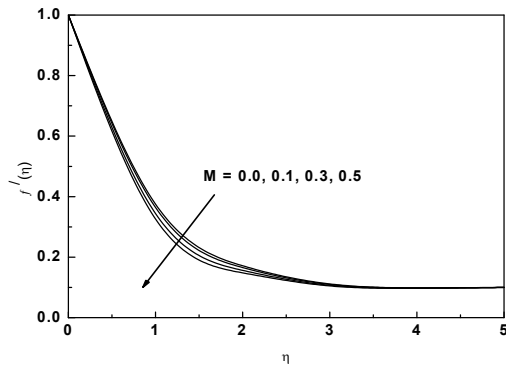


Fig. 2. Velocity Profiles for different values of  $M$ .

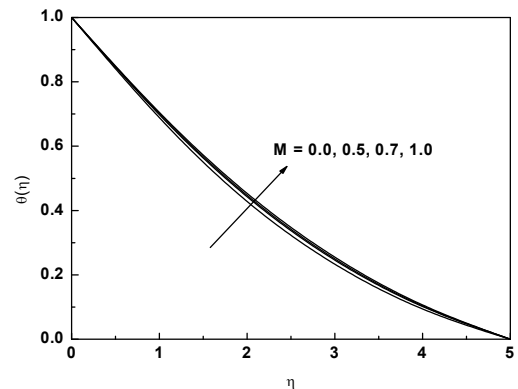


Fig. 3. Temperature profiles for different values of  $M$ .

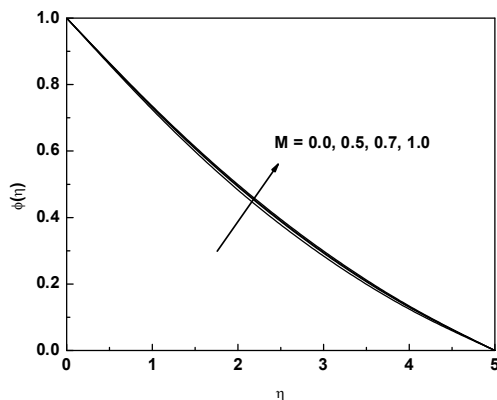


Fig. 4. Concentration profiles for different values of  $M$ .

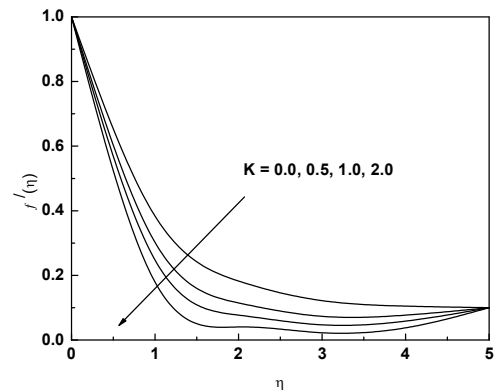
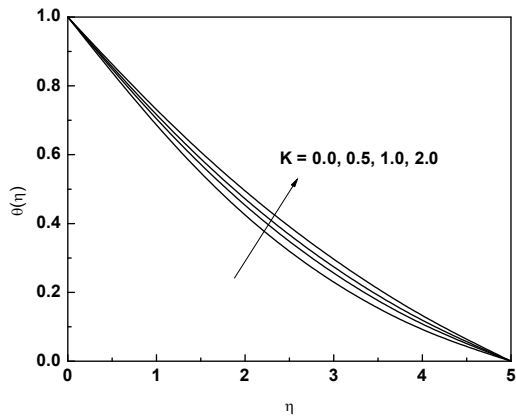
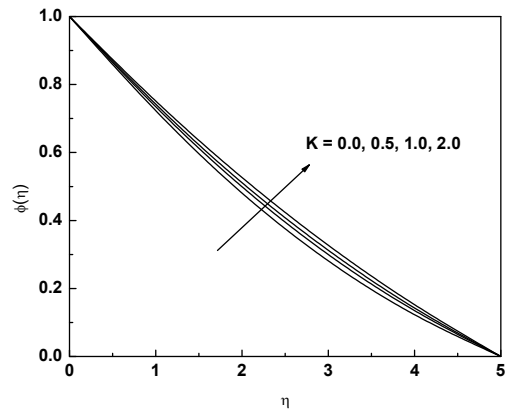


Fig. 5. Velocity profiles for different values of  $K$ .



**Fig. 6.** Temperature profiles for different values of  $K$ .



**Fig. 7.** Concentration profiles for different values of  $K$ .

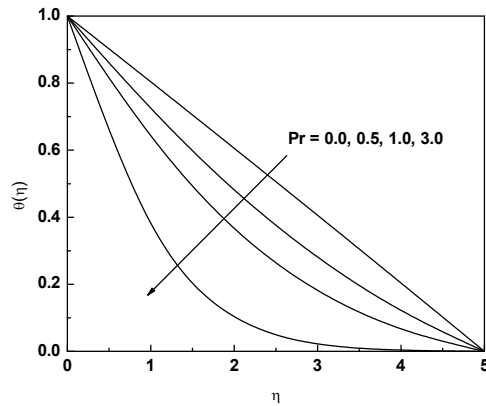


**Fig. 8.** Temperature profiles for different values of  $Pr$ .

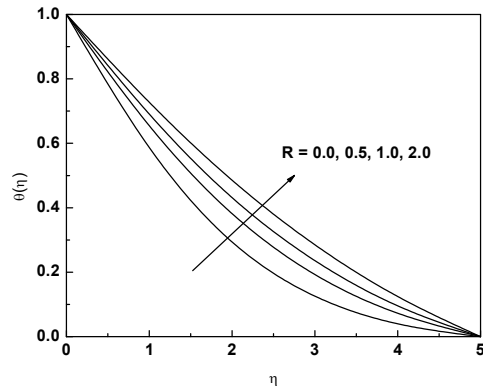


**Fig. 9.** Temperature profiles for different values of  $R$ .

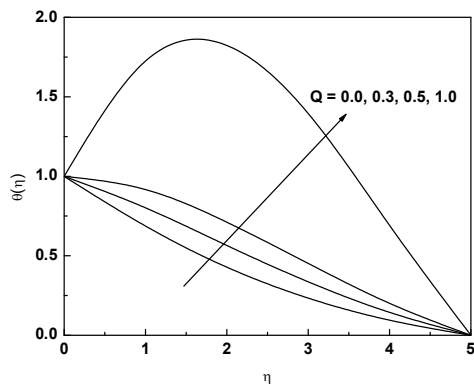


**Fig. 10.** Temperature profiles for different values of  $Q$ .

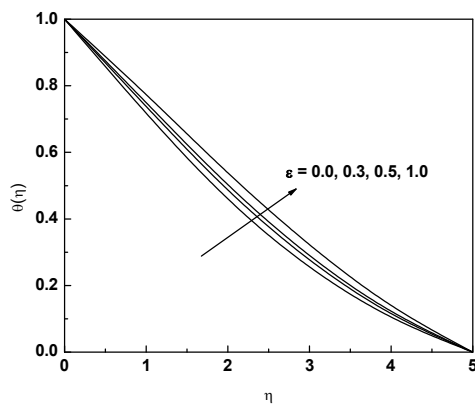


**Fig. 11.** Temperature profiles for different values of  $\epsilon$ .



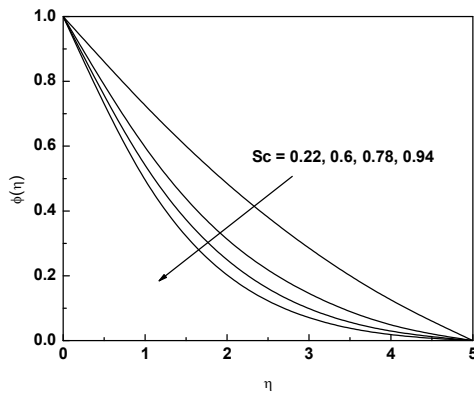


Fig. 12. Concentration profiles for different values of  $Sc$ .

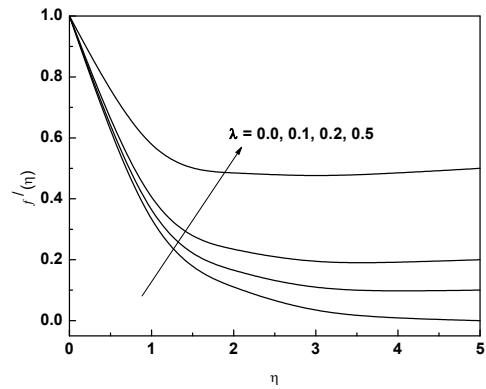


Fig. 13. Velocity profiles for different values of  $\lambda$ .

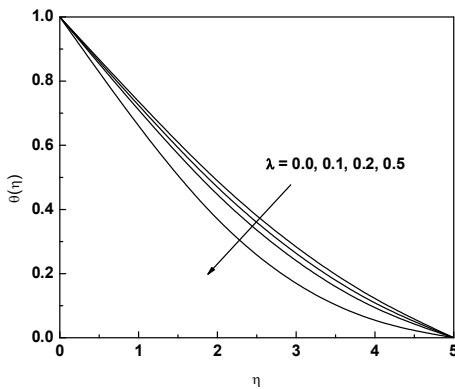


Fig. 14. Temperature profiles for different values of  $\lambda$ .

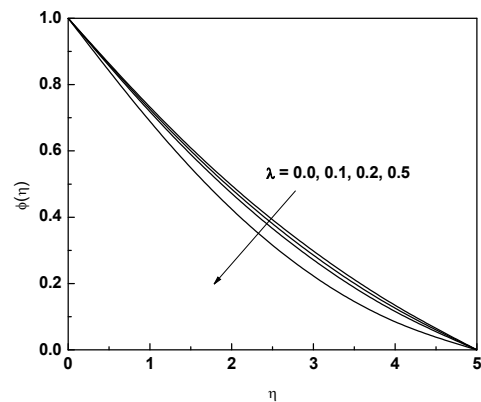


Fig. 15. Concentration profiles for different values of  $\lambda$ .

Table 1. Comparison of skin-friction coefficient  $f''(0)$  for different values of  $\lambda$  and  $M=0.0$ .

$\lambda$	$f''(0)$			
	Pop et al. [26]	Mahapatra and Gupta [20]	Al-sudais [32]	Present paper
0.1	-0.9694	-0.9694	-0.969705	-0.969385
0.2	-0.9181	-0.9181	-0.918349	-0.9181065
0.5	-0.6673	-0.6673	-0.6674611	-0.667261
2.0	2.0174	2.0175	2.01728138	2.0174904

Table 2. Comparison of the Nusselt number  $-\theta'(0)$  for different values of  $\lambda$  when  $M = Q = R = \varepsilon = 0.0, Pr = 0.05$ .

$\lambda$	$-\theta'(0)$			
	Pop et al. [26]	Mahapatra and Gupta [20]	Al-sudais [32]	Present paper
0.1	0.081	0.081	0.080547	0.081241
0.5	0.135	0.136	0.135358	0.135575
2.0	0.241	0.241	0.241025	0.241029

**Table 3.** Numerical values of the skin-friction coefficient, Nusselt number and Sherwood number for  $Pr = 0.71$ ,  $R = 1.0$ ,  $Q = 0.1$ ,  $\varepsilon = 0.1$ ,  $Sc = 0.22$ .

$M$	$K$	$\lambda$	$C_f$	$Nu$	$Sh$
0.1	0.1	0.1	-1.0602	0.268904	0.281977
0.3	0.1	0.1	-1.13321	0.262853	0.279277
0.5	0.1	0.1	-1.20198	0.257454	0.276908
0.1	0.3	0.1	-1.15376	0.257789	0.276929
0.1	0.5	0.1	-1.2398	0.248276	0.272698
0.1	0.1	0.3	-0.934202	0.304593	0.299526
0.1	0.1	0.5	-0.747837	0.344163	0.320372

**Table 4.** Numerical values of the skin-friction coefficient, Nusselt number and Sherwood number for  $M = 0.1$ ,  $K = 0.1$ ,  $\lambda = 0.1$ .

$Pr$	$R$	$Q$	$\varepsilon$	$Sc$	$C_f$	$Nu$	$Sh$
0.71	1.0	0.1	0.1	0.22	-1.0602	0.268904	0.281977
1.0	1.0	0.1	0.1	0.22	-1.0602	0.306422	0.281977
2.0	1.0	0.1	0.1	0.22	-1.0602	0.45044	0.281977
0.71	2.0	0.1	0.1	0.22	-1.0602	0.241735	0.281977
0.71	3.0	0.1	0.1	0.22	-1.0602	0.229604	0.281977
0.71	1.0	0.3	0.1	0.22	-1.0602	0.147114	0.281977
0.71	1.0	0.5	0.1	0.22	-1.0602	0.0723633	0.281977
0.71	1.0	0.1	0.3	0.22	-1.0602	0.236927	0.281977
0.71	1.0	0.1	0.5	0.22	-1.0602	0.20495	0.281977
0.71	1.0	0.1	0.1	0.6	-1.0602	0.268904	0.434922
0.71	1.0	0.1	0.1	0.94	-1.0602	0.268904	0.566934

**6. Conclusions**

In the present investigation, the effect of mass transfer on MHD mixed convection of steady fluid flow along a stretching sheet with variable thermal conductivity was studied in a porous medium with heat generation and thermal radiation. The governing boundary layer equations were transformed into a non-dimensional form and the resulting nonlinear system of partial differential equations was reduced to local non-similarity boundary layer equations, which were solved numerically using Runge-Kutta fourth order technique along with shooting method. It can be drawn from the present results that, when radiation parameter increased, the heat transfer rate at the sheet decreased. It is seen that the Sherwood number increased as an increase in the Schmidt number. Also, the boundary layer flows were greatly influenced by the Prandtl number; as the

Prandtl number increased, the sheet temperature gradients also increased. However, the temperature profiles decreased when the Prandtl number increased. Fluid velocity profiles decreased, whereas temperature and concentration profiles increased with an increase in magnetic field parameter.

**References**

[1] L. J. Crane, "Flow past a stretching plate," *Zeitschrift für Angewandte Mathematik und Physik*, Vol. 21, No. 4, pp. 645-647, (1970).  
 [2] K. B. Pavlov, "Magnetohydrodynamic flow of an incompressible viscous fluid caused by the deformation of a plane surface," *Magnetohydrodynamics*, Vol. 10, pp. 146-148, (1974).  
 [3] H. I. Andersson, "MHD flow of a viscoelastic fluid past a stretching

- surface,” *Acta Mechanica*, Vol. 95, No. 1-4, pp. 227-230, (1992).
- [4] S. Mukhopadhyay, G. C. Layek and S. A. Samad, “Study of MHD boundary layer flow over a heated stretching sheet with variable viscosity,” *International Journal of Heat and Mass Transfer*, Vol. 48, No. 21-22, pp. 4460-4466, (2005).
- [5] K. Bhattacharyya and G. C. Layek, “Chemically reactive solute distribution in MHD boundary layer flow over a permeable stretching sheet with suction or blowing,” *Chemical Engineering Communications*, Vol. 197, No. 12, pp. 1527-1540, (2010).
- [6] H. Tabaei, M. A. Moghimi, A. Kimiaefar and M. A. Moghimi, “Homotopy analysis and differential quadrature solution of the problem of free-convective magnetohydrodynamic flow over a stretching sheet with the Hall effect and mass transfer taken into account,” *Journal of Applied Mechanics and Technical Physics*, Vol. 52, No. 4, pp. 624-636, (2011).
- [7] A. M. Salem and R. Fathy, “Effects of variable properties on MHD heat and mass transfer flow near a stagnation point towards a stretching sheet in a porous medium with thermal radiation,” *Chinese Physics*, Vol. 21, Article ID 054701, (2012).
- [8] I. C. Mandal and S. Mukhopadhyay, “Heat transfer analysis for fluid flow over an exponentially stretching porous sheet with surface heat flux in porous medium,” *Ain Shams Engineering Journal*, Vol. 4, No. 1, pp. 103-110, (2013).
- [9] B. C. Sakiadis, “Boundary layer behavior on continuous solid surfaces: I The Boundary layer equations for two-dimensional and axi-symmetric flow”, *AIChE J.* Vol. 7, No. 1, pp. 26-28, (1961).
- [10] L. E. Erickson, L.T. Fan and V. G. Fox, “Heat and mass transfer on a moving continuous flat plate with suction and injection”, *Industrial & Engineering Chemistry Fundamentals*, Vol. 5, No. 1, pp. 19-25, (1966).
- [11] F. K. Tsou, F. M. Sparrow and R. J. Goldstein, “Flow and heat transfer in the boundary layer in continuous moving surface”, *International Journal of Heat Mass Transfer*, Vol. 10, No. 2, pp. 219-235, (1967).
- [12] A. Noghrehabadi, R. Pourrajab and M. Ghalambaz, “Effect of partial slip boundary condition on the flow and heat transfer of nanofluids past stretching sheet prescribed constant wall temperature,” *International Journal of Thermal Sciences*, Vol. 54, No. 1, pp. 253-261, (2012).
- [13] A. Noghrehabadi, R. Pourrajab and M. Ghalambaz, “Flow and heat transfer of nanofluids over stretching sheet taking into account partial slip and thermal convective boundary conditions”. *Heat Mass Transfer*, Vol. 49, No. 9, pp. 1357-1366, (2013).
- [14] K. Hiemenz, “Die grenzschicht an einem in den gleich formigen flussigkeitsstrom eingetauchten geraden kreiszylinder”. *Dingler's. Polytech. Journal*, Vol. 326, pp. 321-328, (1911).
- [15] F. Homann, “Der Einfluss grosser Zahigkeit bei der Stromung um den Zylinder und um die Kugel”. *Zeitschrift für Angewandte Mathematik und Mechanik*, Vol. 16, No. 3, pp. 153-164, (1936).
- [16] S. I. Pai, “*Viscous Flow Theory I: Laminar Flow*”, D Van Nostrand Company, Inc., New York, (1956).
- [17] H. Schlichting, “*Boundary Layer Theory*”. McGraw- Hill Book Company, New York, (1968).
- [18] J. L. Bansal, “*Viscous Fluid Dynamics*”. Oxford & IBH Publisher Company, New Delhi, (1977).
- [19] T. C. Chiam, “Stagnation-point flow towards a stretching plate,” *Journal of the Physical Society of Japan*, Vol. 63, No. 6, pp. 2443-2444, (1994).
- [20] T. R. Mahapatra and A. S. Gupta, “Magnetohydrodynamic stagnation point

- flow towards a stretching surface”. *Acta Mechanica*, Vol. 152, No. 1-4, pp. 191-196, (2001).
- [21] R. Nazar, N. Amin, D. Filip and I. Pop, “Unsteady boundary layer flow in the region of the stagnation point on a stretching sheet”. *International Journal of Engineering & Science*, Vol. 42, No. 11-12, pp. 1241-1253, (2004).
- [22] W. M. Kay, “Convective Heat and Mass Transfer”, *McGraw-Hill Book Company*, New York, (1966).
- [23] M. Arunachalam and N. R. Rajappa, “Forced convection in liquid metals with variable thermal conductivity and capacity”. *Acta Mechanica*, Vol. 31, No. 1-2, pp. 25-3, (1978).
- [24] L. J. Grubka and K. M. Bobba, “Heat transfer characteristics of a continuously stretching surface with variable temperature”. *Transactions of ASME Journal of Heat and Mass Transfer*, Vol. 107, pp. 248-250, (1985).
- [25] T. C. Chaim, “Heat transfer in a fluid with variable thermal conductivity over stretching sheet”, *Acta Mechanica*, Vol. 129, No. 1-2, pp. 63-72, (1998).
- [26] S. R. Pop, T. Grosan and I. Pop, “Radiation effect on the flow near the stagnation point of a stretching sheet”, *Technische Mechanik*, Vol. 25, No. 2, pp. 100-106, (2004).
- [27] M. A. Hossain and H. S. Takhar, “Radiation effect on mixed convection along a vertical plate with uniform surface temperature,” *Heat and Mass Transfer*, Vol. 31, No. 4, pp. 243-248, (1996).
- [28] D. Pal, “Heat and mass transfer in stagnation-point flow towards a stretching surface in the presence of buoyancy force and thermal radiation”, *Meccanica*, Vol. 44, No. 2, pp. 145-158, (2009).
- [29] P. Vyas and N. Srivastava, “Radiative MHD flow over a non-isothermal stretching sheet in a porous medium”, *Applied Mathematical Sciences*, Vol. 4, No. 50, pp. 2475-2484, (2010).
- [30] H. A. Attia, “Stagnation point flow towards a stretching surface through a porous medium with heat generation”. *Turkish Journal of Engineering and Environmental Sciences*, Vol. 30, No. 5, pp. 299-306, (2006).
- [31] P. R. Sharma and G. Singh, “Effects of variable thermal conductivity and heat source/sink on MHD flow near a stagnation point on a linearly stretching sheet”. *Journal of Applied Fluid Mechanics*, Vol. 2, No. 1, pp. 13-21, (2009).
- [32] N. S. Al-Sudais, “Thermal radiation effects on MHD fluid flow near stagnation point of linear stretching sheet with variable thermal conductivity”. *International Mathematical Forum*, Vol. 7, No. 51, pp. 2525-2544. (2012).
- [33] A. Noghrehabadi, M. R. Saffarian, R. Pourrajab and M. Ghalambaz, “Entropy analysis for nanofluid flow over a stretching sheet in the presence of heat generation/absorption and partial slip”, *Journal of Mechanical Science and Technology*, Vol. 27, No. 3, pp. 927-937, (2013).
- [34] M. Q. Brewster, “Thermal radiative transfer and properties”. New York: John Wiley & Sons, (1992).
- [35] S. D. Conte and C. Boor, “Elementary Numerical Analysis”, *McGraw-Hill Book Company*, New York, (1981).
- [36] M. K. Jain, “Numerical Solution of Differential Equations”, Wiley Eastern Ltd., New Delhi, India, (1984).
- [37] M. K. Jain, S. R. Iyengar and R. K. Jain, “Numerical Methods for Scientific and Engineering Computation”. *Wiley Eastern Ltd.*, New Delhi, India, (1985).
- [38] E. V. Krishnamurthy and S. K. Sen, “Numerical Algorithms”, Affiliated East-West Press Pvt. Ltd., New Delhi, India, (1986).